J. theor. Biol. (1995) **177**, 199–213

Natural Tolerance in a Simple Immune Network

VERA CALENBUHR†‡‖, HUGUES BERSINI‡, JOHN STEWART§ AND FRANCISCO J. VARELA†

† *CREA, Ecole Polytechnique, 1, rue Descartes, F-75005 Paris, France*
‡ *IRIDIA, Université Libre de Bruxelles, C.P. 194/6, 50, Ave. F. Roosevelt, B-1050 Bruxelles, Belgique*
§ *Unité d'Immunobiologie, Institut Pasteur, 25, Rue du Dr. Roux, F-75724 Paris, France*

(*Received on* 3 *October* 1994, *Accepted in revised form on* 28 *April* 1995)

The following basic question is studied here: In the relatively stable molecular environment of a vertebrate body, can a dynamic idiotypic immune network develop a natural tolerance to endogenous components? The approach is based on stability analyses and computer simulation using a model that takes into account the dynamics of two agents of the immune system, namely B-lymphocytes and antibodies. The study investigates the behavior of simple immune networks in interaction with an antigen whose concentration is held constant as a function of the symmetry properties of the connectivity matrix of the network. Current idiotypic network models typically become unstable in the presence of this type of antigen. It is shown that idiotypic networks of a particular connectivity show tolerance towards auto-antigen without the need for *ad hoc* mechanisms that prevent an immune response. These tolerant network structures are characterized by aperiodic behavior in the absence of auto-antigen. When coupled to an auto-antigen, the chaotic attractor degenerates into one of several periodic ones, and at least one of them is stable. The connectivity structure needed for this behavior allows the system to adopt particular dynamic concentration patterns which do not lead to an unbounded immune response. Possible implications for the understanding of autoimmune disease and its treatment are discussed.

1. Introduction

This paper is concerned with the following fundamental question: Can a dynamic idiotypic immune network which develops in the relatively stable somatic molecular environment develop a natural tolerance to endogenous components? And if so, what are the mechanisms for this tolerance? An answer to the second question is vital for gaining insight into what the simplest possible system with self-tolerance looks like. Natural tolerance to endogenous components is central to an organism-centered view of the immune system: that is, here the immune system is seen as being centrally responsible for a somatic identity, and only secondarily to a defensive role (Varela & Coutinho, 1991; Varela *et al.*, 1993; Tauber, 1994). Natural tolerance is also a contentious issue in the classical clonal-selection view of the immune system. In recent years, the interest in the understanding of idiotypic networks has produced a number of models and significant insights (De Boer & Perelson, 1990; Varela & Coutinho, 1991). In these models the dynamics (of soluble and cellular fractions) and meta-dynamics (turnover of clones and new recruitment) of the network have been emphasized. The network's interaction with an external antigen (Ag) has been studied with several degrees of sophistication, but the Ag has always been considered as an infectious agent controlled by the network dynamics (De Boer & Hogeweg, 1989; Neumann & Weisbuch, 1992*a*, *b*; Weisbuch *et al.*, 1993). By adding an Ag, new types of molecules are introduced, whose dynamics have to be considered by adding terms in the equations or by adding new equations, if necessary.

‖ Author to whom correspondence should be addressed at Institut für Medizinische Informatik, Statistik und Epidemiologie Universität Leipzig, Liebig Str. 27, D-04103 Leipzig, Germany. e-mail: Calenbuhr@imise.uni-leipzig.de.

0022-5193/95/230199 + 15 $12.00/0

A question of primary importance is whether tolerance towards auto-Ag can be achieved by the diversity of dynamical configurations or regimes (the dynamical repertoire†) that the model can display when some stable auto-Ag‡ are considered. That is, we study bifurcations of the system to attain bounded response of a perturbed clone. This problem has previously been treated only with simplified cellular automata (Stewart & Varela, 1991). The case of continuously present Ag, a situation corresponding to the one found in auto-Ag and possibly in auto-immune disease, has not been dealt with in full dynamical detail. The exception is Detours *et al.* (1994), which shows how a model taking into account meta-dynamics evolves to an attractor where the shape-space is divided into two zones, which are characterized by high and low levels of antibodies, i.e. a responsive and a tolerant zone, respectively. A constant Ag introduced into the high-level zone of antibodies (Ab's) causes an unbounded immune response, i.e. the system explodes. If the Ag is introduced into the low-level zone, the system can coexist with the Ag. However, this "tolerant" result is obtained only with parameter values that lead to fixed-point attractors. With parameter values such that Ab levels fluctuate, which is likely to be the more realistic situation, the introduction of a (constant) auto-Ag in significant concentration always leads to an unbounded immune response. This model is thus unable to provide a convincing explanation of natural tolerance.

In previous studies in which the perturbation of the system is achieved through interaction with a non-constant, external Ag one usually also starts from a situation in which the unperturbed system's attractors are characterized by different concentration levels of the clones (e.g. Neumann & Weisbuch, 1992*a*, *b*). In this study we approach the problem the othe way round. Our model displays different types of dynamics as a function of the connectivity of the idiotypes. Our starting point will be a chaotic regime which is characterized by the dynamical equivalence of the clones. We show that the interaction of the system's constituents in this chaotic regime with a continuously present and constant Ag causes a degeneration of the chaotic attractor into an attractor in which the clones are no longer equivalent. Instead of launching an unbounded immune response, the system is reciprocally stabilized with the constant Ag.

In this paper we focus on the interaction of a constant Ag with simple immune systems (i.e. with few clones) with basic network structure. The parameter values chosen give rise to the richest behavior compared to other regions in parameter space. For completeness we start with the network model without coupling with auto-Ag, and continue with a discussion of the one-, two- and three-clone cases of the model embedded in a somatic environment of one auto-Ag. In spite of its simplicity, this study case displays some very interesting flexibility that illuminates the spontaneous origin of natural tolerance.

2. The Model

2.1. BASIC MODEL WITHOUT INTERACTIONS

The model was originally proposed by Varela *et al.* (1988) and discussed in Varela & Stewart (1990) and Stewart & Varela (1990). We have since used a slightly modified version of this model, by the use of differently shaped activation functions. Despite its simplicity the model shows a rich dynamical behavior, notably the occurrence of oscillations and chaos (Bersini, 1992; Calenbuhr *et al.*, 1993; Calenbuhr & Bersini, 1993; Bersini & Calenbuhr, 1995). Similar models have been intensively studied by De Boer *et al.* (1993*a*, *b*).

Our model describes the interactions between a soluble and a cellular compartment of variable V-regions, whose behaviors are described by the following differential equations:

$$\frac{df_i}{dt} = -k_1\sigma_i f_i - k_2 f_i + k_3 mat(\sigma_i) b_i \qquad (1)$$

$$\frac{db_i}{dt} = -k_4 b_i + k_5 prol(\sigma_i) b_i + k_6 \quad i = 1, \ldots, n, \qquad (2)$$

where f_i denotes the concentration of the i-th type (clone) of antibody, b_i the population of the i-th type (clone) of B-lymphocytes. The first term in (1) describes the kinetics of the formation of antibody–antibody complexes, the second term accounts for the rate of inactivation of Ab's and the third term describes the production of Ab's by B-cells (B-cell maturation). The first term in (2) accounts for the death-rate of B-cells, the second term for the proliferation of B-cells and the third term represents the production of B-cells in the bone marrow.

The antibody–antibody and antibody–B-lymphocyte interactions are specified by the connectivity matrix M, whose entries $m_{i,j}$ determine whether (antibody or lymphocyte) species i interacts with

† We use the term "dynamical repertoire" to refer to all dynamical regimes that the system can have. Hence dynamical repertoire must not be confounded with the standard use of repertoire, repertoire size, etc., in immunology.

‡ By a stable auto-Ag we understand an Ag that can stimulate the immune system and whose concentration is always held constant.

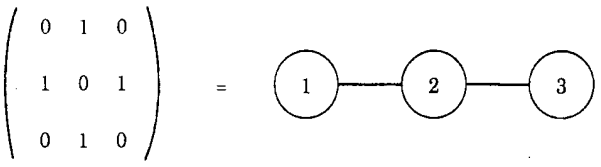

FIG. 1. Connectivity matrix and the corresponding interaction scheme for the three-clone open-chain case.

species j and define the function, σ_i, which is called the field:

$$\sigma_i = \sum_j m_{ij} f_j \tag{3}$$

The term $-k_1 \sigma_i f_i$ represents the formation of $Ab_i Ab_j$ complexes. Although this complex formation is reversible, i.e. the reaction $Ab_i + Ab_j \leftrightarrow Ab_i Ab_j$, it is believed to have its equilibrium on the right-hand side. We will restrict the analysis here to Boolean affinities, such as the ones obtained empirically by ELIZA measurements (Stewart & Varela, 1989): an entry "1" in the connectivity matrix (CM) indicates a threshold affinity between clones f_i and f_j, while a "0" indicates the absence of affinity. For example, a situation where all members react only with their nearest neighbors results in a CM in which all elements are zero except for the direct-neighbor elements of the diagonal. We will refer to that case as the open chain case (see Figs 1 and 2 for the three-clone case). Adding non-zero corner elements to this matrix is equivalent to closing the chain of interaction.

The functions mat and prol determine how B-cells mature and proliferate upon activation:

$$\text{mat}(\sigma_i) = \exp - \left\{ \frac{\ln(\sigma_i/\mu_m)}{s_m} \right\}^2 \tag{4}$$

$$\text{prol}(\sigma_i) = \exp - \left\{ \frac{\ln(\sigma_i/\mu_p)}{s_p} \right\}^2 \tag{5}$$

The parameter values for the results presented here are as follows: $k_1 = 0.0016[\text{conc}^{-1}\,\text{d}^{-1}]$; $k_2 = 0.02[\text{d}^{-1}]$; $k_3 = 2.0[\text{d}^{-1}]$; $k_4 = 0.1[\text{d}^{-1}]$; $k_5 = 0.2[\text{d}^{-1}]$; $k_6 = 0.1[\text{d}^{-1}]$; $\mu_m = 80[\text{conc}^2]$; $s_m = 0.5$; $\mu_p = 120[\text{conc}^2]$; $s_p = 0.5$.

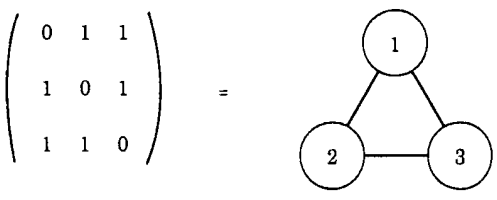

FIG. 2. Connectivity matrix and the corresponding interaction scheme for the three-clone closed-chain case.

In the one-clone case the system has one fixed point, but oscillations appear in the two-clone case. Various types of behavior are found for the three-clone case, namely oscillations (open chain) and chaos (closed chain). In brief, in the absence of Ag, the three-clone case consists of six coupled ordinary differential equations. The basic behavior of this system including meta-dynamics has been discussed in Stewart & Varela (1991) and Detours *et al.* (1994).

2.2. COUPLING WITH AN AUTO-AG

The coupling of an Ag whose concentration remains constant is the simplest way of representing an autologous antigen. From the mathematical point of view it introduces the least modification at the level of the equations. For this case (3) is replaced by

$$\sigma_i = \sum_{k=1}^{k=n'} l_{i,k} \text{Ag}_k + \sum_{j=1}^{j=n} m_{i,j} f_j, \tag{6}$$

where Ag_k denotes an auto-Ag coupled to the network via the interaction matrix l. In the following discussion we will drop all indices with the understanding that there is always only one auto-Ag present. Only in the three-clone open-chain case do we need to specify with which clone the Ag interacts.

A fixed auto-Ag corresponds to a situation of a molecule that is always immediately being replenished. One can imagine this to be the case for abundant molecules (possibly on cells) circulating freely in the environment. Although low concentrations of Ag are often found in the case of auto-Ag, it is by no means the only hypothesis to claim that their concentration is constant, as some fluctuations might also be present. The condition: [Ag] = constant is most likely satisfied by molecules on tissues. Strictly speaking, however, in the present formulation we would have a problem with our equations since this would require the inclusion of terms that account for reactions on two-dimensional surfaces, i.e. flow terms and the degree of coverage of the tissue by the Ab. We do not treat this case here but concentrate on the simpler scenario described earlier.

Although mathematically simple, a constant Ag is the hardest possible perturbation for the system, and one most likely to lead to an unbounded immune response. As will be shown in Section 3.1, with the parameter values employed here, the critical case for the one-clone system is when the auto-Ag concentration is in the range $\mu_m \approx 80 \leqslant [\text{Ag}] \leqslant 180 \approx [\text{Ag}_c]$, where it will explode. For the two-clone system the critical range is smaller, since the perturbed clone receives additional stimulation from the unperturbed clones raising its mean field faster into a region where the activation functions decrease. The range of the

critical region depends on the parameter values and the number of clones and their interaction scheme.

2.3. COMPUTATIONAL ASPECTS

The system equations were integrated using a fourth-order Runge–Kutta method with adaptive step size. It is important to note that the solutions with auto-Ag are different from the solutions without auto-Ag as the coupling of an auto-Ag to the network leads to a new attractor. The time series shown in the following sections were usually obtained by initially integrating the system equations without auto-Ag interaction and then adding a constant Ag. We shall refer to the integration time without Ag as the delay, which must not be confounded with the usual meaning of delay-terms in the context of differential equations. In this way the different attractors in the two situations are easily appreciated. The bifurcation analysis, however, is based on calculations and simulations with the auto-Ag present from the very beginning. We have given parameter values and initial conditions in Appendices A, B and C, enabling the reader to reproduce the time-series plots with delay in the different regimes, as shown in the figures.

An often-heard question alludes to the concern of possibly reaching different attractors in the situation with and without delay. This concern is justified only to a certain degree. The reason being the following: in principle, the system has the same attractors once the auto-Ag is present. However, if we allow for a delay, the last values of the variables before the introduction of Ag correspond to the initial conditions of the system with Ag. In the two-clone and three-clone systems the predominant behavior (for the parameters chosen) are oscillations and aperiodic behavior. In general, one cannot be sure whether the initial conditions of the system in the periodic attractors cover the phase-space sufficiently to find all attractors. In the chaotic case, the situation is different as the system's variables cover larger regions in phase-space, although we cannot be sure that they do so sufficiently. Hence, there would be a non-negligible chance of missing some attractors by introducing the Ag after a delay. To avoid this trap we have based our bifurcation diagrams on simulations with random starting conditions and have included simulations with delay only for reasons of visual clarity in the plots of the time series.

Nevertheless, the bifurcation diagrams still do not contain all attractors. We have omitted some attractors as we did not want to overload the diagrams. First, there is always a stable node (all clones die) if the starting concentrations of B-cells and Abs are not sufficiently high. Second, some particular—though very unlikely—starting conditions can give rise to interesting periodic patterns. As these were never found using random starting conditions and since their basins of attraction are very small compared to the ones reported, we have not included them either. Third, there is always a chance of missing an attractor with a very small basin of attraction.

2.4. GENERAL STRUCTURE OF THE PAPER

In the following, we shall study the behavior of the system as a function of its network structure with and without perturbation, i.e. with auto-Ag interaction and without it. We will discuss the results obtained for the one-, two-, and three-clone case and discuss the stability diagrams of these systems as a function of the control parameter [Ag]. The stability diagrams show the mean concentration of the perturbed clone as a function of [Ag]. In this way the impact of the Ag on the actual dynamics of the system can be appreciated.

As we shall see, there is a certain range of [Ag] in which the one-clone and two-clone systems have an unbounded immune response. For the one-clone system this unstable regime occurs in a large window of the parameter [Ag]. For the two-clone and three-clone systems, however, we shall see that this critical zone leading to instability lies, roughly speaking in the range $\mu_m < [Ag] < \mu_p$. The basic question that we address is whether the immune system can cut the response towards a constant Ag solely due to its dynamic repertoire without the need for explicit mechanisms. In the three-clone closed chain case, in which aperiodic behavior is found, the system has a means to access an attractor in which the interaction with auto-Ag does not lead to an unbounded immune response.

3. Results

3.1. THE ONE-CLONE CASE

A one-clone system is much less artificial than it may appear at first glance. In the classical Burnetian view of clonal selection theory it is assumed that the immune system is driven by external antigens, and that reactions between antibodies of different types are absent. From that point of view the one-clone case discussed here is merely the response one would expect from any clone being excited by a constant Ag. From the point of view of second-generation immune networks (Varela & Coutinho, 1991) the one-clone case corresponds to a clone isolated from the rest of the

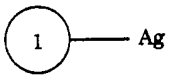

FIG. 3. Interaction of the one-clone system with Ag.

network, with some potential implications for autoimmunity.

For the one-clone case the system is described just by two equations:

$$\frac{df}{dt} = -k_1\sigma f - k_2 f + k_3 \text{mat}(\sigma) b \tag{7}$$

$$\frac{db}{dt} = -k_4 b + k_5 \text{prol}(\sigma) b + k_6 \tag{8}$$

and the field $\sigma(i)$ reduces in this case to a parameter, i.e. $\sigma = [\text{Ag}]$. The position of the steady states depend on σ, and are:

$$f^0 = \frac{[k_3 \text{mat}(\sigma)(-k_6)]}{\{[-k_4 + k_5 \text{prol}(\sigma)][k_1\sigma + k_2]}$$

$$b^0 = \frac{-k_6}{[-k_4 + k_5 \text{prol}(\sigma)]}$$

If no auto-Ag is present the steady state is at $(f^0, b^0) = (0.0, k_6/k_4)$. Linearization of (7) and (8) about the steady states gives the Jacobian

$$A = \begin{bmatrix} -k_1 - k_2\sigma & k_3 \text{mat}(\sigma) \\ 0 & -k_4 + k_5 \text{prol}(\sigma) \end{bmatrix} \tag{9}$$

For the solution of the characteristic equation corresponding to (9) one finds the following results. The trace $\text{Tr} = (-k_1 - k_2\sigma - k_4 + k_5 \text{prol}(\sigma))$ is always negative. The determinant $\det = (-k_2 - k_1\sigma)(-k_4 + k_5 \text{prol}(\sigma))$ is negative if $k_4 > k_5 \text{prol}(\sigma)$, implying stability. Hence, for $\sigma < 79.14$ and $\sigma \geqslant 181.96$ the system has two real negative eigenvalues, i.e. stable nodes. For $79.14 \leqslant \sigma < 181.96$ one positive and one negative eigenvalue are found, hence a saddle point.

The introduction of a fixed antigen provokes the production of Ab's and the proliferation of B-cells. In the unstable region, the system's behavior is dominated by the third term in (7) due to the exponential growth of the maturation function.

In a certain range of the parameter [Ag] the system is always stable. That means that a small variation of the concentration of the auto-Ag will be damped out. In these regions the system can couple naturally with an auto-Ag. By increasing [Ag] into the unstable region, the system will explode. Nevertheless, the system can cope with a large range of Ag-concentrations without becoming unstable.

The solution for the fixed auto-Ag also gives us some clues for other cases. The most important of them is where a fixed amount of external Ag that has no intrinsic dynamics and that can be removed by interaction with Abs is injected into the system. We expect that the system always returns to its fixed point

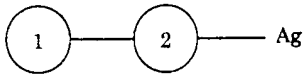

FIG. 4. Interaction of the two-clone system with Ag.

in the stable regions. Moreover, in the unstable region the system will launch a strong immune response that removes the Ag. As soon as the injected quantity has been sufficiently reduced, the system will return to its stable regime.

3.2. THE TWO-CLONE CASE

Without auto-Ag the two clones oscillate out of phase and have the same amplitude [Fig. 5(a)]. With low [Ag] an asymmetry is introduced such that the perturbed clone oscillates in a higher concentration range and the other one in a reduced range [Fig. 5(b)]. When increasing the auto-Ag concentration the asymmetry becomes more pronounced: the perturbed clone oscillates at ever larger amplitudes and the other

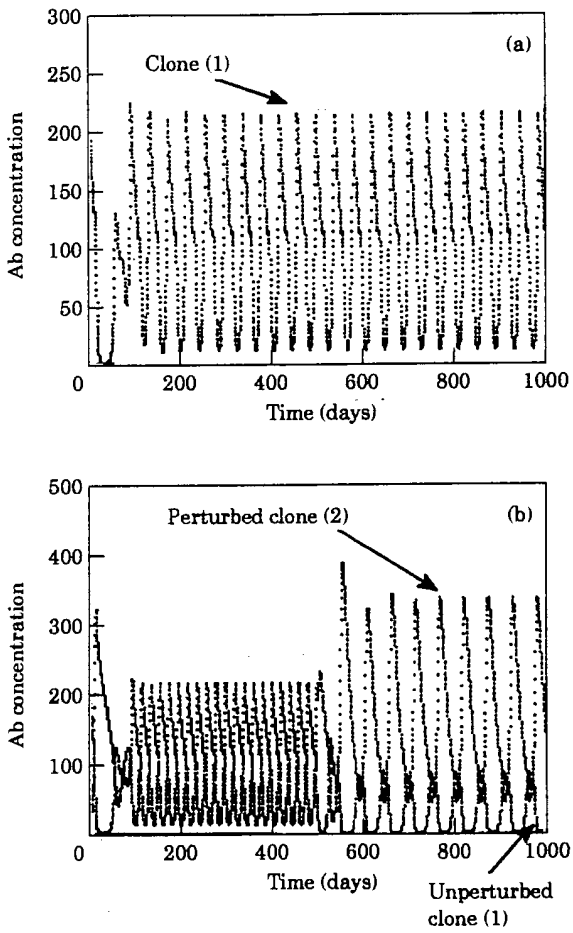

FIG. 5. (a) Time series of the first clone of the unperturbed two-clone system, i.e. without Ag. (b) Time series of the second clone of the perturbed two-clone system. The Ag is introduced after 500 days, [Ag] = 50.

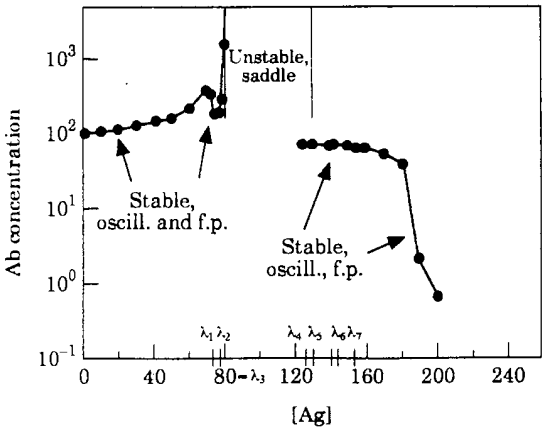

FIG. 6. Bifurcation diagram of the two-clone system. The mean concentration of the perturbed clone is plotted as a function of the Ag concentration. f.p. = fixed point. The dotted line denotes stable branches. The following types of behavior were found: with Ag $0 \leqslant [Ag] \leqslant \lambda_1 = 72.42$; oscillations, $\lambda_1 = 72.42 < [Ag] < \lambda_2 = 77.28$, stable focus, $\lambda_2 = 77.28 \leqslant [Ag] < \lambda_3 \approx 79.1$, stable node; $\lambda_3 \approx 79.1 \leqslant [Ag] < \lambda_4 = 124.91$, saddle. Up to this value of [Ag] arbitrary starting conditions in the range 0–300 for the Ab's and 0–60 for the B-lymphocytes can be used. For $\lambda_4 = 124.91 \leqslant [Ag] < \lambda_5 = 136.97$, there is coexistence of a saddle and a stable periodic regime. The vertical bars denote the approximate boundaries of the critical zone. The saddle can be found using starting conditions $f_1 = 5.528$, $f_2 = 276.178$, $b_1 = 16.578$, $b_2 = 25.371$; the limit cycle can be found using starting conditions $f_1 = 43.827$, $f_2 = 37.529$, $b_1 = 20.610$, $b_2 = 59.05$. Note that different starting conditions can lead to slightly different values of the bifurcation points. For $136.97 \leqslant [Ag]$ arbitrary starting conditions in the range 0–300 for the Ab's and 0–60 for the B-lymphocytes can be used. For $\lambda_5 = 136.97 \leqslant [Ag] < \lambda_6 = 140.7$, limit cycle oscillations; $\lambda_6 = 140.7 \leqslant [Ag] < \lambda_7 = 154.75$, stable focus, $\lambda_7 = 154.75 \leqslant [Ag]$, stable node. Simulations were carried out in all cases with Ag present from the very beginning.

one at smaller ones. At [Ag] = 72.42 a bifurcation point is reached and the oscillatory regime is transformed into a stable focus (Fig. 6). Again, the perturbed clone attains a fixed concentration at a higher level than the unperturbed one. At [Ag] = 77.28 the stable focus becomes a stable node until eventually, at $\mu_m \approx [Ag] \approx 79.1$, a saddle is reached where the perturbed clone grows unbounded and the unperturbed one dies off. Increasing [Ag] further, one reaches a region with two coexisting regimes in phase space: a saddle and a stable limit cycle. The oscillatory regime is characterized by non-overlapping concentration levels of the two clones, with the perturbed clone oscillating at higher levels than the unperturbed clone. An increase in Ag levels leads to a reduction of the amplitudes of oscillation until eventually a stable focus is reached which turns into a stable node with even higher [Ag] levels. The concentrations reached by the clones converge toward zero.

3.3. THE CLOSED-CHAIN THREE-CLONE CASE

The three clone case is interesting because it represents the simplest network with more than one interaction possibility. We begin with the three-clone closed-chain case (3-ccc case), as illustrated in Fig. 7. In the absence of auto-Ag the system displays aperiodic behavior [Fig. 8(a)]. We refer to this regime as type 0. Observing the dynamics of simulations one gets the impression the system is continuously trying to form pairs of clones that synchronize (as is the case in the three-clone open-chain case, see below). However, as soon as a new pair is forming they break up and a new attempt is made to form a pair with the other clone. The clones participating in the pair formation are selected randomly and the attempts to form a pair occur irregularly. From a dynamical point of view, all the clones are equivalent or interchangeable, a consequence of closing the chain of interaction. The phenomenon just described is reminiscent of frustration phenomena found in neural networks (Atiya & Baldi, 1989; Marcus *et al.*, 1991) and spin glasses (Toulouse, 1977) and was therefore named "frustration induced chaos". A complete description appears in Bersini & Calenbuhr (1995).

It can be shown that this type of chaos can be reached via an intermittent route by changing the parameter k_3 in (1) (Calenbuhr & Bersini, 1993). The laminary phases of the intermittent regime are characterized by high-level, large-amplitude oscillations of a pair of clones and low-level, small-amplitude oscillations of the other clone. All clones can participate in these high-level and low-level oscillations. The amplitudes of the clone oscillating in the low-concentration range increase as a function of time until the concentration range of the other two clones are reached. At this point the chaotic phase starts again until, after a certain while, another clone starts oscillating in the low concentration range. For even smaller values of k_3 the system displays oscillations that resemble the laminary phase type. They are different in that the amplitude of the clone oscillating in the low-level range remains constant.

We start our discussion of the impact of an auto-Ag on the 3-ccc case for parameter values that lead to chaotic type-0 behavior. This will be essential for the further discussion of the impact of an auto-Ag on the system in the intermittent and oscillatory regime.

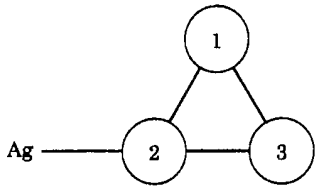

FIG. 7. Interaction of clone 2 with Ag in the 3-ccc case.

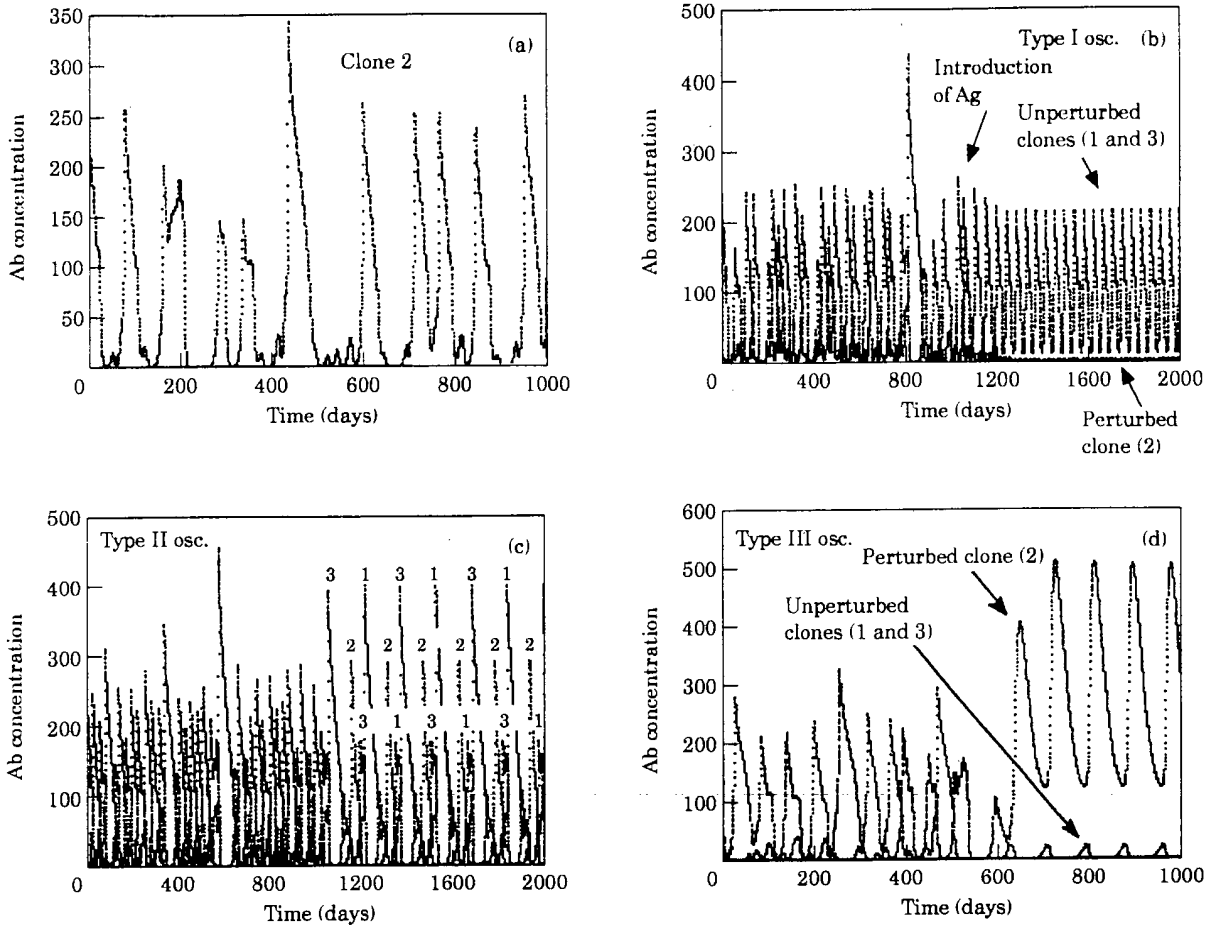

FIG. 8. (a) Time series of the second clone in the unperturbed 3-ccc case. (b) Time series of the perturbed 3-ccc case. The Ag is introduced at $t = 1000$ days. [Ag] = 10. (c) Time series of 3-ccc case. The [Ag] = 40 is introduced at $t = 1000$ days. (d) Time series of the 3-ccc case. The Ag (=70) is introduced at $t = 500$ days.

The introduction of an auto-Ag leads to several changes in the behavior of the system. We first give a brief overview of the different types of behavior found; more detailed analyses and exact parameter values for which bifurcations occur are given in Appendix A. For small values of [Ag] the chaotic regime persists. From a critical value onwards, the chaotic attractor degenerates into a periodic attractor. Roughly speaking, for two values, $[Ag^i] < \mu_m$ and $[Ag^i] > \mu_p$, the system is always stable. That means that the presence of Ag neither leads to an unbounded increase of one of the clones nor is any of them totally suppressed. For $\mu_m < [Ag^i] < \mu_p$ (the critical region) the system has one stable regime (bounded response) and one unstable regime (unbounded response). In the following we shall discuss the mechanisms that enable the system to display a bounded response in the presence of auto-Ag.

The system undergoes several bifurcations and changes of stability as a function of the auto-Ag concentration [Fig. 9(a); Appendix A], and has three dynamical regimes that coexist in some regions of parameter space of the control parameter [Ag]. These regimes are referred to as branch I, branch II and branch III, respectively. Each of these regimes is distinguished by a characteristic oscillation which we refer to as type I, type II and type III, respectively. Moreover, on branch III we also find fixed points that replace the type-III oscillation when increasing the control parameter. Appendix A contains a detailed description of this intricate bifurcation diagram.

We now take a closer look at the system's behavior near the critical range. Type-I oscillations show the following behavior [refer to Fig. 8(b) (the corresponding fixed points have the same concentration patterns)]: the perturbed clone oscillates with low amplitude, while the other two oscillate with a high amplitude. The two non-perturbed clones always have the same concentration and oscillate out of phase with the perturbed one. Further, $\partial\langle[Ab^i]\rangle/\langle\partial[Ag]\rangle < 0$.

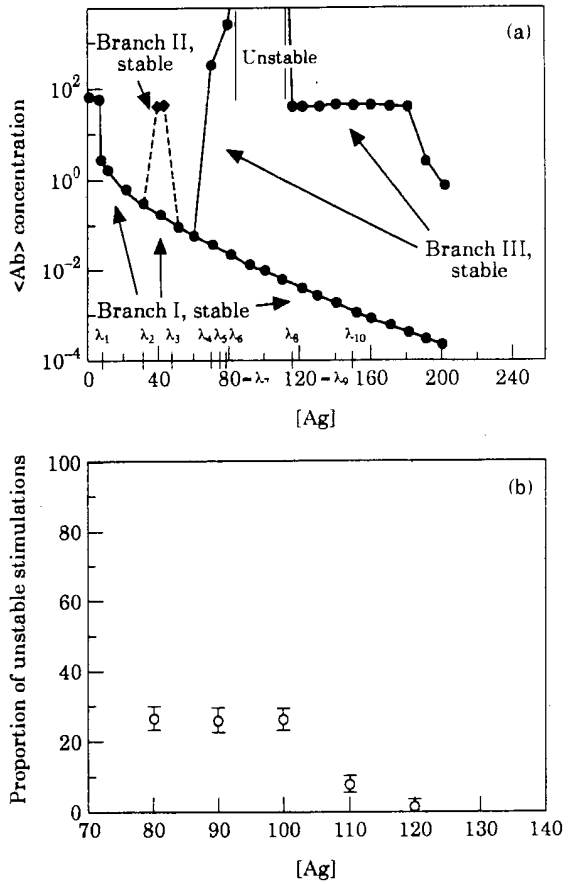

FIG. 9. (a) Bifurcation diagram of the 3-ccc case. The mean concentration of the perturbed clone is plotted as a function of the Ag-concentration. The dotted line denotes stable branches. f.p. = fixed point. The following types of behavior were found: with $0 \leqslant [Ag] < \lambda_1 = 6.69$, chaotic attractor; $\lambda_1 \leqslant [Ag] < \lambda_2 = 36.441$, type-I oscillations; $\lambda_2 = 36.441 \leqslant [Ag] < \lambda_3 = 45.215$, birhythmicity (type-I and type-II oscillations); $\lambda_3 = 45.215 \leqslant [Ag] < \lambda_4 = 69.98$, type-I oscillations; $\lambda_4 = 69.98 \leqslant [Ag] < \lambda_5 = 70.73$, birhythmicity (type-I and type-III oscillations); $\lambda_5 = 70.73 \leqslant [Ag] < \lambda_6 = 78.66$, coexistence of branch I (type-I oscillations) and branch III (stable focus); $\lambda_6 = 78.66 \leqslant [Ag] < \lambda_7 = 79.2$, coexistence of branch I (type-I oscillations) and branch III (stable node); $\lambda_7 = 79.2 \leqslant [Ag] < \lambda_8 = 123.48$, coexistence of branch I (type-I oscillations) and branch III (saddle). The vertical bars denote the approximate boundaries of the critical zone. $\lambda_8 = 123.48 \leqslant [Ag] < \lambda_9 = 149.0$ corresponds to coexistence of branch I (type-I oscillations) and branch III (stable focus); $\lambda_9 = 149.0 \leqslant [Ag]$, coexistence of branch I (type-I oscillations) and branch III (stable node). For a detailed description of the types of behavior found, see Appendix A. (b) Proportion of simulations leading to branch III. We have run 10 × 200 simulations with 2000 random starting conditions.

The laminary phase of the unperturbed 3-ccc system is in many respects similar to the type-I regime.

The type-III oscillations are characterized by large-amplitude oscillations of the perturbed clone and low-amplitude oscillations of the unperturbed clones. The perturbed clone oscillates out of phase with the perturbed clones [Fig. 8(d)]. Branches I and III thus have the inverse concentration patterns. While the perturbed clone on branch I has a low concentration, the perturbed clone on branch III has a high concentration. Branch I remains stable, while branch III becomes unstable in the critical zone. The coupling of an Ag to the unperturbed system leads the aperiodic attractor to degenerate into a periodic one. The system has at least two choices: a stable or an unstable regime.

Different starting conditions lead to one of the two possible branches. In the beginning of the critical zone, i.e. for $[Ag] \approx \mu_m$, we find that about one quarter of all starting conditions gives rise to trajectories on branch III. The basin of attraction becomes smaller with increasing [Ag], as seen from the results in Fig. 9(b). We have tried to characterize the starting conditions leading to either one of the branches and have found none. It appears that there are no preferred starting conditions leading to either one regime. This is reminiscent of riddled basins of attraction (Alexander *et al.*, 1992; Sommerer & Ott, 1993; Ott *et al.*, 1993). It is beyond the scope of this article to investigate this aspect further. If the arbitrariness with which either of the attractors can be reached should turn out to be a more general phenomenon, i.e. if it should be characteristic of larger systems, then it is a question that should be investigated more seriously for its medical implications.

3.4. THE OPEN-CHAIN THREE-CLONE CASE

In the absence of any antigen clones 1 and 3 always oscillate in phase and have the same concentration, while clone 2 oscillates in phase opposition. The amplitude of clone 2 is twice as large as that of clone 1 or 3 (Fig. 10).

The difference with the perturbed three-clone closed-chain case is that we have to distinguish two cases. The auto-Ag can perturb one of the clones at the end of the chain, i.e. clone 1 or 3, or (i) it can perturb clone 2. We discuss the second case first.

Introduction of an auto-Ag leads to an oscillatory regime which is similar in behavior to type-III oscillations in that the perturbed clone oscillates out of phase with clones 1 and 3 and with higher amplitude (Fig. 12). We refer to this type of behavior as type-IV oscillations. Appendix B contains a more detailed description of the behavior, which is shown in Fig. 13. Suffice to mention that for $[Ag^i] < \mu_m$ and $[Ag^i] > \mu_p$, the system is always stable. That means that the presence of Ag neither leads to an unbounded increase of one of the clones nor are any of them totally suppressed. At $[Ag^i] = 78.84$ (i.e. $[Ag^i] \approx \mu_m$) a bifurcation occurs, which transforms the stable node into a saddle characterized by an unbounded increase of the perturbed clone and death of the unperturbed ones. At $[Ag^i] = 116.98$ (i.e. $[Ag^i] \approx \mu_p$) a bifurcation occurs, which transforms the saddle point into a stable

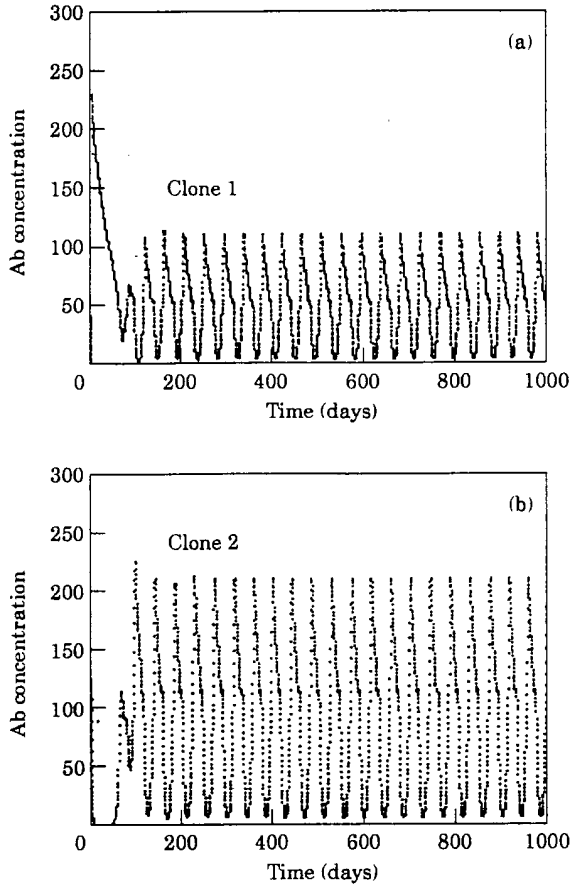

FIG. 10. Time series of the unperturbed 3-coc system. (a) Clone 1; (b) clone 2.

focus, leading to a bounded response of the perturbed clone again.

We now turn to the perturbation of either one of the end clones (clone 1 to fix ideas).

In what we have discussed so far, there has always been symmetry between clones 1 and 3. In the present configuration, this is no longer the case. For most values of the parameter [Ag], the three clones have different concentration levels. The results found are shown in Fig. 15 and are described in Appendix C. For this case we find a bifurcation that transforms a stable node into a saddle at the beginning of the critical range, which leads to an unbounded immune response of the perturbed clone, while the two others die. At the end

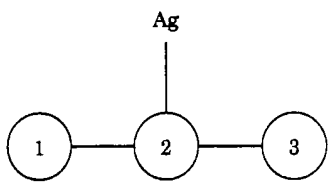

FIG. 11. Coupling of the central clone in the 3-coc case.

of the critical zone, the system has several coexisting regimes, among them stable ones.

The essence of the results just described are summarized in Table 1. The study of three basic cases has illustrated how the system can avoid an unbounded immune response in a physiological concentration range provided the system operates in or near a chaotic regime, in which case the system does not need an *ad hoc* mechanism to stop an explosive immune response.

4. Discussion

4.1. SCALING AND DYNAMICAL CONTROL

The idiotypic network models studied to date do not have explicit mechanisms that stop short an immune response in the presence of a constant Ag. The fundamental question that we addressed here is different: namely, whether it is possible to have a coherent co-existence between the network and a constant somatic auto-Ag solely on the basis of the dynamic repertoire of the system. We have seen that at least in the three-clone closed-chain case, the system has a means for coping with this type of Ag. One mechanism to avoid an unbounded response is the degeneration of a chaotic attractor into one of several possible periodic attractors, one of which is tolerant. In general, the 3-ccc system can avoid an unbounded response by adopting particular concentration patterns that characterize attractors that are not accessible to systems with less connected structures of the connectivity matrix.

The interpretation of this result is related to the impression that in the absence of Ag the system is continuously trying to form pairs of clones that synchronize in high level oscillations, the third clone being relegated to low level oscillations. The amplitude of the "low" clone increases in time until the concentration range of the "high" clones is reached and the system enters a chaotic phase. Over a long time period, the three clones are dynamically equivalent. It seems the introduction of an auto-Ag breaks this three-way symmetry. In one of the attractors, the stable one, the perturbed clone is designated for the role of low-level oscillations. In the other attractor, the unstable one, the perturbed clone shows high-level concentrations.

In order to better understand why one of the possible concentration patterns leads to a stable situation, let us look again at the one-clone case. The stability analysis has shown that there is a range of [Ag] for which the system has a positive and a negative eigenvalue. This result can be generalized. It does not matter whether the field received by one clone is generated by one or

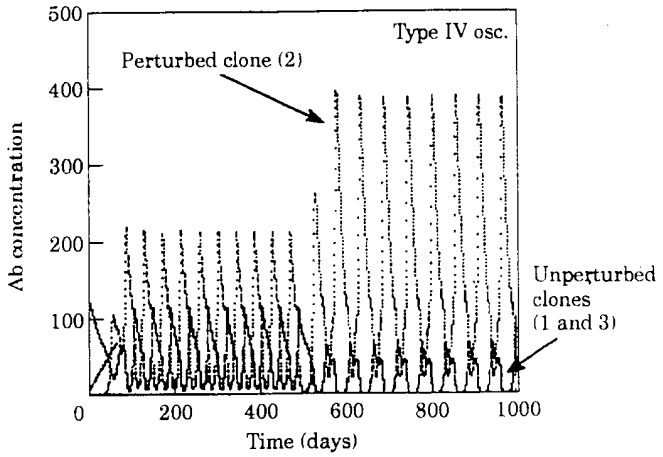

FIG. 12. Time series of the perturbed 3-coc system. The Ag (=40) is introduced at t = 500 days.

many Ags or by Ag + Abs. Only the field received matters. We have already noted that in the one-clone case the hardest perturbation is met when a constant auto-Ag is in the concentration range $\mu_m \approx [Ag] \leqslant [Ag_c]$. Since in this case the perturbed clone does not receive additional stimulation from other clones, which could raise its mean field to $[Ag_c]$, it will explode. We may, therefore, predict that tolerance will be easier to achieve the closer the auto-Ag concentration is to $[Ag_c]$, since the additional field required is correspondingly less. This qualitative expectation is confirmed by the results presented here, since we may observe that unbounded immune responses always occur in the auto-Ag range immediately above μ_m.

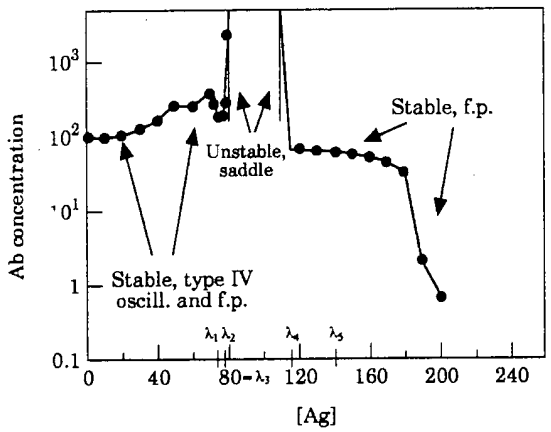

FIG. 13. Bifurcation diagram of the 3-coc system, auto-Ag coupled to the middle clone 2. The mean concentration of the perturbed clone is plotted as a function of the Ag concentration. f.p. = fixed point. The dotted line denotes stable branches. The following types of behavior were found: with $0 \leqslant [Ag] < \lambda_1 = 72.35$, type-IV oscillations; $\lambda_1 = 72.35 \leqslant [Ag] < \lambda_2 = 77.23$, stable focus; $\lambda_2 = 77.23 \leqslant [Ag] < \lambda_3 = 78.84$, stable node; $\lambda_3 = 78.84 \leqslant [Ag] < \lambda_4$, saddle-point. The vertical bars denote the approximate boundaries of the critical zone. For $\lambda_4 = 116.98 \leqslant [Ag] < \lambda_5 = 155.75$, stable focus; $\lambda_5 = 155.75 \leqslant [Ag]$, stable node. For a detailed description of the types of behavior found, see Appendix B.

Since the three-clone closed-chain configuration reliably provides a strong additional field for the perturbed clone from the two high-level clones, the conditions are met for stabilizing the system in a tolerant mode even for auto-Ag concentrations in the critical range. Hence, the present study gives us some clues as to how the dynamic repertoire of a small immune system can provide similar behavior as that of natural immune networks in the presence of a diversity of somatic auto-Ag which are relatively constant in concentration. This result is particularly suggestive in the light of the recent reports of both narrow-band and broad-band fluctuations in natural populations and antibodies in mice and men (Lundqvist *et al.*, 1989; Varela *et al.*, 1991). Whether these natural fluctuations are a reflection of natural tolerance remains to be determined.

The next logical step is to simulate higher dimensional systems and draw conclusion about how well this behavior scales up with size. One could attribute the behavior of the 3-ccc system solely to the network architecture ostensibly responsible for the various dynamical regimes that underlie the co-existence with constant auto-Ag. However, a detailed study of the dynamics as a function of the type of connectivity matrix for much larger systems (up to ca. 50 clones) has shown that the system can also display many different chaotic regimes, among them intermittent ones. Whether chaotic or (through parameter dependence) related intermittent and oscillatory

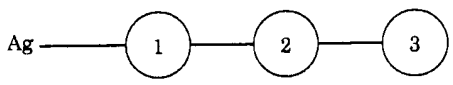

FIG. 14. Interaction of clone 1 with Ag in the 3-coc case.

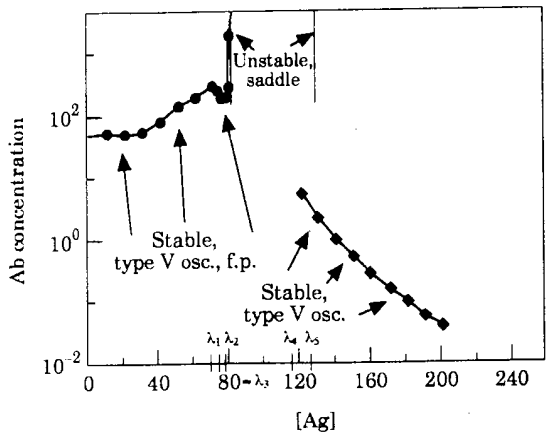

FIG. 15. Bifurcation diagram of the 3-coc system with the Ag acting upon clone 1 (perturbation leads to similar behaviour of clone 3). The mean concentration of the perturbed clone is plotted as a function of the Ag concentration. f.p. = fixed point. The dotted line denotes stable branches. The following types of behavior were found: with $0 \leqslant [Ag] < \lambda_1 = 72.52$, type-V oscillations; $\lambda_1 = 72.52 \leqslant [Ag] < \lambda_2 = 77.02$, stable focus; $\lambda_2 = 77.02 \leqslant [Ag] < \lambda_3 = 79.1$, stable node; $\lambda_3 = 79.1 \leqslant [Ag] < \lambda_4 = 114.41$, saddle. The vertical bars denote the approximate boundaries of the critical zone. For $\lambda_4 = 114.41 \leqslant [Ag] < \lambda_5 = 127.10$, coexistence of a saddle and type-V oscillations; $\lambda_5 = 114.41 > [Ag]$, type-V oscillations. For a detailed description of the types of behavior found, see Appendix C.

regimes that the model can generate might behave in the same way as in the 3-ccc case, is a question that cannot be answered yet. We are currently conducting a systematic study of this question and found that at least intermittent regimes of larger systems can also coexist with auto-Ag (Calenbuhr *et al.*, in preparation).

The biggest obstacle to the study of higher dimensional systems is our current ignorance of realistic connectivity matrices beyond a few empirical studies (Stewart & Varela, 1989; B-Rao & Stewart, unpublished). What is needed is some sort of building block whose behavior is well understood and which puts us in a position to study higher dimensional systems in more economic ways than just integrating $2n$-equations with n large. The 3-ccc case may turn out to relate to those building blocks of the connectivity matrix which allow us to predict, at least on empirical grounds, the qualitative behavior of larger systems.

TABLE 1

Summary of results

These are the basic types of behavior for the three different type of networks studied:

- Two-clone case without Ag: oscillations;
- Two-clone case with Ag: oscillations; system becomes unstable for certain concentration ranges of the Ag;
- Three-clone open-chain case without Ag: oscillations;
- Three-clone open-chain case with Ag: oscillations; system becomes unstable for certain concentration ranges of the Ag;
- Three-clone closed-chain case without Ag: chaos;
- Three-clone closed-chain case with Ag: chaotic attractor degenerates into several dynamic regimes of lower complexity, at least one of which is always stable in the presence of auto-Ag.

The degeneration of the chaotic attractor into a periodic one upon coupling the system to an Ag is reminiscent of several attempts of controlling chaos. A chaotic attractor can be considered a collection of a large number of unstable periodic attractors. Controlling chaos usually involves the selection of one of these unstable periodic attractors and its stabilization. The type of chaos displayed by the present system has been named frustration induced chaos due to the similarity with frustration induced changes of behavior in neural networks (Bersini & Calenbuhr, 1995). Frustration induced chaos is distinguished by the dynamical equivalence of each of the three variables on both time scales (B-cell and Ab timescale, respectively). Interesting applications of the control of frustration induced chaos will be reported elsewhere (Calenbuhr & Bersini, in preparation).

4.2. TOLERANCE AND AUTOIMMUNITY

We have seen that the 3-ccc case leads to at least two major attractors in the presence of auto-Ag: a stable one and an unstable one. Can we draw from these results any useful insight with respect to the etiologies of autoimmune disease and their treatment?

According to our network interpretation, autoimmune disease could be due to defects in the network structure (Varela & Coutinho, 1991). In particular, intravenous injection of pooled Ig (IvIg) is a successful clinical practice which could be explained by a camouflage- or fill out-effect of the network defects (Kaveri *et al.*, 1991). Further, in a case study of a patient suffering from Hashimoto's thyroiditis we have shown the changes in network dynamics before and after IvIg treatment (Dietrich *et al.*, 1993). Autoimmune patients often display remission of symptoms after IvIg treatment, but the symptoms recur after a couple of months.

Our simple model shows that it might be possible to move the system—in the multi-stable regime—from one attractor to another by applying an appropriate perturbation. This would also take us closer to an understanding of the mechanisms of some autoimmune diseases in terms of coexisting dynamic regimes. Clearly the 3-ccc case is far too simple, and provides only a suggestive possibility for larger dimensional systems moving to and from unstable and stable branches under perturbations. It may be doubted whether the unstable branch has any direct relevance for the understanding of auto-immune disease since a system does not remain in an unstable attractor for long. However, a trajectory on the unstable attractor can be part of a heteroclinic orbit

and end up in another stable attractor, which corresponds in our case either to a large production of Abs or to a large production of Abs that could be removed by a mechanism that is not yet included in our model. The shift could, in principle, be from the stable to the unstable regime or, alternatively, the system is being shifted from an attractor corresponding to a large Ab-production to the stable attractor. After the application of the perturbation, the system will go along on that attractor. Recall that coexisting attractors cannot only be reached by applying a perturbation but also by starting from different initial conditions. If the initial conditions, i.e. the concentrations of the Abs produced in the bone marrow, correspond to those that lead to the attractor responsible for an autoimmune state, then we would expect that after a while the attractor that has been reached through the application of a perturbation will again be replaced by the autoimmune one.

The appealing simplicity of the model in its present version and the fact that many different dynamic regimes can be easily reached by changing symmetry properties of the interaction architecture gives us some hope that tolerance may be achieved using the dynamic repertoire inherent to the model.

4.3. PREVIOUS MODELS

How do the results of this study compare to other models? In the 3-ccc case, all Abs are equivalent. We observe the same behavior irrespective of which clone is perturbed by the Ag. As we have seen, this type of response is only possible in this particular situation. The problem of model network's behavior towards continuously present Ag has also been investigated by Detours *et al.* (1994). Their model differs in some respects from the one discussed here, since it focuses on morphogenetic effects in shape-space including meta-dynamics, i.e. an updated variable list of clones occurs on a slower timescale than that of the dynamics. The model has a bounded dynamics if and only if the parameters governing the system dynamics are chosen in such a way that one has a fixed point. In this situation the shape space is partitioned, as a result of the system's development, into two zones: one high zone in which the clones are present in relatively low concentrations and where they are under a high field and another low zone in which the clones are present in high concentrations and are under a low field. In our case, we also find high and low level zones—albeit oscillating ones—but these regimes emerge in continuous interaction with a constant Ag, while Detours *et al.* consider an autonomous dynamic followed by perturbation from a constant Ag when both zones are already constituted.

We have already suggested that it is the equivalence of clones in the chaotic regime that endows the system with the capacity to tolerate auto-Ag. The closed-chain situation, however, is inconsistent with Detours *et al.*, since one needs multiple epitopes for a closed chain, while only complementary shapes are admitted in their model. We conclude that the biologically realistic case with multiple epitopes is an important consideration to take into account in immune network models.

To our knowledge, the present study and the paper by Detours *et al.* are the only ones that deal with continuously present auto-Ag. The interaction of immune system models with an external, variable Ag as in classical immune responses, has been dealt with in several ways. An interesting case is the Caylee tree model first introduced by Weisbuch *et al.* (1990) and further developed by Weisbuch *et al.* (1993) and Neumann & Weisbuch (1992*a*, *b*). We refer to this model as the Weisbuch–De Boer–Perelson model (WBP). In the WBP model, "tolerant" and "immunized" states result from the autonomous system dynamics and not from the interaction with an Ag, which is introduced as perturbations after stability. Upon introduction of an Ag, these fixed point attractors are modified but they remain qualitatively unchanged. Neumann & Weisbuch (1992*b*) also investigated the impact of the topology on the system's response towards external Ag. They found that odd loops (which correspond to the 3-ccc case) also favor tolerance. Our results, although obtained using a different model and different Ag-dynamics, point in the same direction.

4.4. FUTURE STUDIES

There is a need to study (simplified) higher-dimensional systems. Also, we have to test the robustness of our results when relaxing the constraint of Boolean type affinities. In addition, would a system with meta-dynamics select those interaction schemes favoring the stable regimes in presence of constant Ag? Finally, the concentrations of auto-Ags are often small compared to the normal concentrations of Abs in the (unperturbed) system, which is what we have studied here. It would also be interesting to study the system's behavior in contact with other auto-Ags having different types of dynamics and found in other concentration ranges (Calenbuhr *et al.*, in preparation).

VC gratefully acknowledges financial support from the Fritz-Thyssen Stiftung. The authors would like to thank the members of the Paris-Brussels group in theoretical immunology—in particular A. Coutinho—for many discussions.

REFERENCES

ALAMGIR, M. & EPSTEIN, I. (1983). Birhythmicity and compound oscillation in coupled chemical oscillators: chlorite-bromate-iodide system. *J. Am. Chem. Soc.* **105,** 2500–2502.

ALEXANDER, J. C., YORKE, J. A., YOU, Z. & KAN, I. (1992). Riddled basins. *Int. J. Bifurcation & Chaos*, **2,** 795–813.

ATIYA, A. & BALDI, P. (1989). Oscillations and synchronizations in neural networks: an exploration of the labeling hypothesis. *Int. J. Neural Syst.* **1,** 103–124.

BERSINI, H. (1992). The interplay between the dynamics and metadynamics of the immune network. In: *Artificial Life III* (Langton, C., ed.). Addison-Wesley.

BERSINI, H. & CALENBUHR, V. (1995). Frustration induced chaos in a system of coupled ODE's. *J. Chaos, Solitons & Fractals* **5**(8), 1533–1549.

CALENBUHR, V., BERSINI, H., VARELA, F. J. & STEWART, J. (1993). The impact of the structure of the connectivity matrix on the dynamics of a simple model for the immune network. In: *Proceedings of the 1st Copenhagen Symposium on Computer Simulation in Biology, Ecology and Medicine* (Mosekilde, E., ed.).

CALENBUHR, V. & BERSINI, H. (1993). Frustration induced chaos and intermittency. IRIDIA Technical Report, Université Libre de Bruxelles.

DE BOER, R. & HOGEWEG, P. (1989). Unreasonable implications of reasonable idiotypic network assumptions. *Bull. math. Biol.* **51,** 381–408.

DE BOER, R. & PERELSON, P. (1990). Size and connectivity as emergent properties of a developing immune network. *J. theor. Biol.* **149,** 381–424.

DE BOER, R., KEVREKIDIS, I. G. & PERELSON, A. S. (1993*a*). Immune network behaviour I: from stationary states to limit cycle oscillations. *Bull. math. Biol.* **55,** 745–780.

DE BOER, R., KEVREKIDIS, I. G. & PERELSON, A. S. (1993*b*). Immune network behaviour I: from oscillations to chaos and stationary states. *Bull. math. Biol.* **55,** 781–816.

DECROLY, O. & GOLDBETER, A. (1982). Birhythmicity, chaos, and other patterns of temporal self-organization in a multiply regulated biochemical system. *Proc. natn. Acad. Sci. U.S.A.* **79,** 6917–6921.

DETOURS, V., BERSINI, H., STEWART, J. & VARELA, F. J. (1994). Development of idiotypic network in shape space. *J. theor. Biol.* **170,** 401–414.

DIETRICH, G., VARELA, F. & KAZATCHKHINE, M. (1993). Manipulating the human immune network with IgG. *Eur. J. Immunol.* **23,** 2945–295[illegible].

KAVERI, S.-V., DIETRICH, G., HUREZ, V. & KAZATCHKINE, M. D. (1991). Intravenous immunoglobulins (IVIg) in the treatment of autoimmune diseases. *Clin. expl Immunol.* **86,** 192–198.

LUNDKVIST, I., COUTINHO, A., VARELA, F. & HOLMBERG, D. (1989). Evidence for the functional dynamics in an antibody network. *Proc. natl. Acad. Sci. U.S.A.* **88,** 5074–5078.

MARCUS, C. M., WAUGH, F. R. & WESTERVELT, R. M. (1991). Nonlinear dynamics and stability of analog neural networks. *Physica D* **51,** 234–247.

NEUMANN, A. U. & WEISBUCH, G. (1992*a*). Window automata analysis of population dynamics in the immune system. *Bull. math. Biol.* **54,** 21–44.

NEUMANN, A. U. & WEISBUCH, G. (1992*b*). Dynamics and topology of idiotypic networks. *Bull. math. Biol.* **54,** 699–726.

OTT, E., GREBOGI, C. & YORKE, J. A. (1990). Controlling chaos. *Phys. Rev. Lett.* **64,** 1196–1199.

OTT, E., SOMMERER, J. C., ALEXANDER, J. C., KAN, I. & YORKE, J. A. (1993). Scaling behaviour of chaotic systems with riddles basins. *Phys. Rev. Lett.* **71,** 4134–4137.

SOMMERER, J. C. & OTT, E. (1993). A physical system with qualitatively uncertain dynamics. *Nature* **365,** 138–140.

STEWART, J. & VARELA, F. (1989). Exploring the connectivity of the immune network. *Immunol. Rev.* **110,** 37–61.

STEWART, J. & VARELA, F. (1990). Dynamics of a class of immune networks. II. Oscillations of the humoral and cellular compartments. *J. theor. Biol.* **144,** 103–115.

STEWART, J. & VARELA, F. (1991). Morphogenesis in shape space: elementary meta-dynamics of immune networks. *J. theor. Biol.* **153,** 477–498.

TAUBER, F. (1994). *The Immune Self. Theory or Metaphor. A Philosophical Inquiry*. Cambridge: Cambridge University Press.

TOULOUSE, G. (1977). Theory of the frustration effect in spin glasses I. *Commun. Phys.* **2.4,** 115–119.

VARELA, F., COUTINHO, A., DUPIRE, B. & VAZ, N. (1988*a*). Cognitive networks: immune, neural, and otherwise. In: *Theoretical Immunology, Part II. SFI Series on the Science of Complexity* (Perelson, A., ed.) New Jersey: Addison Wesley. pp. 359–375.

VARELA, F. & STEWART, J. (1990). Dynamics of a class of immune networks. I. Global stability of idiotype interactions. *J. theor. Biol.* **144,** 93–101.

VARELA, F. & COUTINHO, A. (1991). Second generation immune networks. *Immunol. Today* **12,** 159–167.

VARELA, F., ANDERSON, A., DIETRICH, G., SUNDBLAD, A., HOLMBERG, D., KAZATCHKINE, M. & COUTINHO, A. (1991). Population dynamics of natural antibodies in normal and autoimmune individuals. *Proc. natn. Acad. Sci. U.S.A.* **88,** 5917–5921.

VARELA, F., STEWART, J. & COUTINHO, A. (1993). What is the immune system for? In: *Thinking about Biology. SFI Series* (Stein, W. & Varela, F., eds) New Jersey: Addison Wesley.

WEISBUCH, G., DE BOER, R. J. & PERELSON, A. S. (1990). Localized memories in idiotypic networks. *J. theor. Biol.* **146,** 483–499.

WEISBUCH, G., ZORZENON DOS SANTOS, R. M. & NEUMANN, A. U. (1993). Tolerance to hormones in an idiotypic network model. *J. theor. Biol.* **163,** 237–253.

Appendix A

Analysis of the 3-ccc Phase Portrait

The type-I oscillations show the following behavior [refer to Fig. 8(b)]: the perturbed clone oscillates with low amplitude, while the two others oscillate with a high amplitude. The two non-perturbed clones always have the same concentration and oscillate out of phase with the perturbed one. Further, $\partial\langle[\mathrm{Ab}^i]\rangle/\langle\partial[\mathrm{Ag}]\rangle < 0$. The laminary phase of the unperturbed three-clone closed-chain system is in many respects similar to the type-I regime.

In type-II oscillations, a period-6 attractor, we find large amplitude oscillations of the unperturbed clones and low amplitude oscillations of the perturbed clones [see Fig. 8(c)].

The type-III oscillations are characterized by large-amplitude oscillations of the perturbed clone and low-amplitude oscillations of the unperturbed clones. The perturbed clone oscillates out of phase with the perturbed clones [Fig. 8(d)].

Results may be verified using the starting conditions indicated below and introducing the Ag at $t = 250$ days. In that way, the reader will be enabled to reproduce time series as those that we have represented in the figures. By denoting those values of the bifurcation parameter [Ag] that lead to a bifurcation or a change of stability by λ_i we find the following results:

for $0 \leqslant [\mathrm{Ag}] < \lambda_1 = 6.69$ and arbitrary starting conditions in the range $0 < [f_i] \leqslant 300$ and $0 < [b_i] \leqslant 60$ the chaotic attractor persists.

The mean concentration of the perturbed clone decreases when [Ag] is increased;

for $\lambda_1 \leqslant [\mathrm{Ag}] < \lambda_2 = 36.441$ and arbitrary starting conditions in the range $0 < [f_i] \leqslant 300$ and $0 < [b_i] \leqslant 60$ the chaotic regime degenerates into a periodic one with type-I oscillations;

for $\lambda_2 = 36.441 \leqslant [\mathrm{Ag}] < \lambda_3 = 45.215$: birhythmicity, type-I and type-II oscillations. The bifurcation giving rise to two coexistent limit cycles is similar to a pitchfork bifurcation. Several starting conditions give rise to either one of the regimes, e.g. $f_1 = 203.31$, $f_2 = 186.227$, $f_3 = 216.121$, $b_1 = 15.449$, $b_2 = 58.952$, $b_3 = 7.096$ lead to branch I and $f_1 = 217.125$, $f_2 = 45.770$, $f_3 = 155.556$, $b_1 = 31.808$, $b_2 = 22.124$, $b_3 = 53.206$ lead to branch II. For birhythmicity see Decroly & Goldbeter (1982) and Alamgir & Epstein (1983);

for $\lambda_3 \leqslant [\mathrm{Ag}] < \lambda_4 = 69.98$ and arbitrary starting conditions in the range $0 < [f_i] \leqslant 300$ and $0 < [b_i] \leqslant 60$, only one regime, namely type-I oscillations, is found;

for $\lambda_4 = 69.98 \leqslant [\mathrm{Ag}] < \lambda_5 = 70.73$: birhythmicity. At $\lambda_4 = 69.98 = [\mathrm{Ag}]$ there is again a pitchfork bifurcation for limit cycles, giving rise to type-I and type-III oscillations. Several starting conditions give rise to either one of the regimes, e.g. $f_1 = 166.079$, $f_2 = 94.663$, $f_3 = 117.336$, $b_1 = 16.766$, $b_2 = 8.210$, $b_3 = 22.821$ lead to branch I and $f_1 = 291.801$, $f_2 = 86.241$, $f_3 = 224.374$, $b_1 = 21.304$, $b_2 = 3.16$, $b_3 = 39.021$ lead to branch III. Also, $f_1 = 71.463$, $f_2 = 190.412$, $f_3 = 51.675$, $b_1 = 34.596$, $b_2 = 30.606$, $b_3 = 20.668$ lead to branch III. As was described in Section 3.3 and displayed in Fig. 9(b), the basin of attraction for branch III shrinks with increasing Ag concentration. Note that in the middle of the critical zone the first set of starting conditions giving rise to branch III no longer falls into this basin of attraction, but instead leads to branch I. The second set of starting conditions giving rise to branch III, however, does so before, during and after the critical zone;

for $\lambda_5 = 70.73 \leqslant [\mathrm{Ag}] < \lambda_6 = 78.66$: coexistence of branch I and branch III. At $\lambda_6 = 70.73$ a (reverse) Hopf bifurcation occurs on branch III, transforming the periodic attractor into a stable focus. Either regime can be reached using the same starting conditions as for the case $\lambda_4 = 69.98 \leqslant [\mathrm{Ag}] < \lambda_5 = 70.73$;

for $\lambda_6 = 78.66 \leqslant [\mathrm{Ag}] < \lambda_7 = 79.2$: coexistence of branch I and branch III. On branch III the stable focus is transformed into a stable node. Either regime can be reached using the same starting conditions as for the case $\lambda_4 = 69.98 \leqslant [\mathrm{Ag}] < \lambda_5 = 70.73$;

for $\lambda_7 = 79.2 \leqslant [\mathrm{Ag}] < \lambda_8 = 123.48$: coexistence of branch I and branch III. On branch III, two eigenvalues become positive (corresponding to the perturbed clone and its B-lymphocyte) resulting in a saddle-point and hence instability. This is the only unstable regime found. Starting conditions $f_1 = 71.463$, $f_2 = 190.412$, $f_3 = 51.675$, $b_1 = 34.596$, $b_2 = 30.606$, $b_3 = 20.668$ lead to branch III;

for $\lambda_8 = 123.48 \leqslant [\mathrm{Ag}] < \lambda_9 = 149.0$: coexistence of branch I and branch III. On branch III the saddle is replaced by a stable focus. This stable focus displays the same concentration pattern of the three clones as type-III oscillations, i.e. the perturbed clone has a high concentration and the unperturbed clones have low and the same concentration;

for $\lambda_9 = 149.0$: $\leqslant [\mathrm{Ag}]$ coexistence of branch I and branch III. On branch III the stable focus is transformed into a stable node.

Appendix B

Analysis of the 3-occ Phase Portrait, Ag coupled to Clone 2

Simulations where carried out with random values in the range 0–300 for the Ab's and 0–60 for the B-lymphocytes. As there are no coexisting regimes, results should be easily verified. As one varies the control parameter [Ag] the following regimes are found:

for $0 \leqslant [\mathrm{Ag}] < \lambda_1 = 72.35$: type IV oscillations; at λ_1 a (inverse) Hopf bifurcation occurs and replaces the limit cycle by a stable focus;

for $\lambda_1 = 72.35 \leqslant [\mathrm{Ag}] < \lambda_2 = 77.23$: stable focus;

for $\lambda_2 = 77.23 \leqslant [\mathrm{Ag}] < \lambda_3 = 78.84$: stable node;

for $\lambda_3 = 78.84 \leqslant [\mathrm{Ag}] < \lambda_4$: at λ_3 two eigenvalues become positive (corresponding to the perturbed clone and its B-lymphocyte) resulting in a saddle-point and hence instability: the perturbed clone grows unbounded and the unperturbed clones die in this region of [Ag];

for $\lambda_4 = 116.98 \leqslant [\mathrm{Ag}] < \lambda_5 = 155.75$: stable focus;

for $\lambda_5 = 155.75 \leqslant [\mathrm{Ag}]$: stable node.

Appendix C

Analysis of the 3-occ Phase Portrait, Ag coupled to Clone 1

Here we report only on those regimes that are characterized by relatively large basins of attraction. Results may be verified using the starting conditions indicated below and introducing the Ag at $t = 250$ days. In this way, the reader will be able to reproduce the time series that we have shown in the figures.

For $0 \leqslant [Ag] < \lambda_1 = 72.52$: type-V limit-cycle oscillations. For small values of [Ag] these oscillations are characterized by the following concentration pattern: $\langle[Ab_2]\rangle > \langle[Ab_3]\rangle > \langle[Ab_1]\rangle$. With increasing [Ag], $\langle[Ab_1]\rangle$ becomes larger while $\langle[Ab_2]\rangle$ and $\langle[Ab_3]\rangle$ become smaller until we find the concentration pattern $\langle[Ab_1]\rangle > \langle[Ab_2]\rangle > \langle[Ab_3]\rangle$. There is, however, no abrupt change leading to the dominance of clone 1. The inversion of the concentration pattern takes continuously place in the range $30 < [Ag] < 40$. Moreover, upon increasing [Ag] the period becomes larger. Note that type-V oscillations are neither similar to type-III nor to type-IV oscillations where we have the concentration pattern $\langle[Ab_2]\rangle > \langle[Ab_3]\rangle = \langle[Ab_1]\rangle$. Type V oscillations are characterized by three different concentration levels of the clones. One set of starting conditions leading to this regime is $f_1 = 217.125$, $f_2 = 45.770$, $f_3 = 155.556$, $b_1 = 31.808$, $b_2 = 22.124$, $b_3 = 53.207$.

for $\lambda_1 = 72.52 \leqslant [Ag] < \lambda_2 = 77.02$: stable focus; at $\lambda_1 = 72.52$ an (inverse) Hopf bifurcation occurs, which transforms the limit cycle into a stable focus; same starting conditions as for the case $0 \leqslant [Ag] < \lambda_1 = 72.52$;

for $\lambda_2 = 77.02 \leqslant [Ag] < \lambda_3 = 79.1$: stable node; at $\lambda_2 = 77.02$ the stable focus is replaced by a stable node; same starting conditions as for the case $0 \leqslant [Ag] < \lambda_1 = 72.52$;

for $\lambda_3 = 79.1 \leqslant [Ag] < \lambda_4 = 114.41$: saddle; at $[Ag] < \lambda_3 = 79.1$ two eigenvalues become positive (corresponding to the perturbed clone and its B-lymphocyte) resulting in a saddle-point and hence instability: the perturbed clone grows unbounded and the unperturbed clones die in this region of [Ag]; same starting conditions as for the case $0 \leqslant [Ag] < \lambda_1 = 72.52$;

for $\lambda_4 = 114.41 \leqslant [Ag] < \lambda_5 = 127.10$: coexistence of a saddle and type-V oscillations, which are now characterized by the concentration pattern $\langle[Ab_3]\rangle > \langle[Ab_2]\rangle > \langle[Ab_1]\rangle$. The stable branch can be reached using the same starting conditions as for the case $0 \leqslant [Ag] < \lambda_1 = 72.52$; while the unstable branch can be reached using the following set of starting conditions: $f_1 = 29.382$, $f_2 = 155.749$, $f_3 = 149.313$, $b_1 = 59.426$, $b_2 = 8.583$, $b_3 = 42.268$;

for $\lambda_5 = 114.41 > [Ag]$: type-V oscillations characterized by the concentration pattern $\langle[Ab_3]\rangle > \langle[Ab_2]\rangle > \langle[Ab_1]\rangle$; same starting conditions as for the case $0 \leqslant [Ag] < \lambda_1 = 72.52$.